

◆ EXPERIMENTAL INVESTIGATION ◆

A Comparative Analysis of Bench-Top Performance Assessment of Distal Protection Filters in Transient Flow Conditions

Gail M. Siewiorek, PhD¹; Mark H. Wholey, MD²; and Ender A. Finol, PhD³

¹Institute for Complex Engineered Systems, Carnegie Mellon University, and ²Department of Radiology, University of Pittsburgh Medical Center–Shadyside, Pittsburgh, Pennsylvania, USA.

³Department of Biomedical Engineering, The University of Texas at San Antonio, Texas, USA.

◆ ————— ◆
Purpose: To compare the performance in vitro of 6 distal protection filters (DPFs) on the basis of filtration ability and effects on pressure gradient and vascular impedance in a flow model of the internal carotid artery (ICA).

Methods: Six DPFs (Accunet, Angioguard, FilterWire, Gore Embolic Filter, NAV6, and SpiderFX) were evaluated in a physiologically realistic flow loop. A blood analog was heated to body temperature and circulated by a pulsatile pump outputting a time-varying flow rate representative of the ICA. The ICA flow model was a highly curved tube representing a challenging site for filter deployment. The DPFs were deployed at the apex of the curved segment, and 2 sizes of microspheres (143 and 200 μm) were injected to simulate embolization. The capture efficiency, pressure gradient, normalized pressure gradient, and vascular impedance were calculated.

Results: The Gore filter had high capture efficiency (143 μm : 99.97%; 200 μm : 100.00%) with relatively small increases in pressure gradient (143 μm : +27%; 200 μm : +20%) and vascular impedance (143 μm : +23.4%; 200 μm : +6.1%) after particles were injected. Spider had the lowest capture efficiency (143 μm : 1.50%; 200 μm : 19.34%, $p < 0.0005$), while NAV6 (143 μm : +916%, $p < 0.0005$) and Accunet (200 μm : +179%, $p < 0.0005$) yielded the largest pressure gradient increases.

Conclusion: A bench-top flow apparatus exhibiting physiologically realistic conditions was developed by combining pulsatile flow and a body temperature blood analog. Using microspheres larger than the pore size of most of the DPFs, the device-wall apposition has an important effect on the overall filter performance and the global fluid dynamics in the flow model.

J Endovasc Ther. 2012;19:249–260

Key words: in vitro experiment, flow model, internal carotid artery, stent, embolic protection filter, distal protection, vascular impedance, pulsatile flow

◆ ————— ◆
Distal protection filters (DPFs) were developed for use during carotid artery stenting (CAS) to address concerns that catheter manipulations and stent deployment can

dislodge plaque debris and precipitate a neurological event.^{1,2} The only randomized trial to date comparing CAS with and without cerebral protection was reported by Barbato

This work was supported in part by the American Heart Association and W.L. Gore & Associates, Inc.

Gail M. Siewiorek has no commercial, proprietary, or financial interest in any products or companies described in this article. Mark H. Wholey has disclosed that he is a consultant to Cordis, Abbott (Guidant), Medrad, Boston Scientific, Edwards LifeSciences, and Mallinckrodt. He is also co-founder and Chairman of the Board of Directors for NeuroInterventions, Inc. Ender A. Finol is co-founder and VP of Engineering for NeuroInterventions, Inc.

Corresponding author: Ender A. Finol, PhD, The University of Texas at San Antonio, AET 1.360, One UTSA Circle, San Antonio, TX 78249 USA. E-mail: ender.finol@utsa.edu

et al.³ Although the authors concluded that DPFs demonstrated no reduction in microemboli, the study was conducted on a small

See commentary page 261

number of patients in a single center study (n=36 randomized in a 1:1 scheme). However, the Carotid Revascularization Endarterectomy versus Stenting Trial (CREST) found no overall difference in the primary endpoint (stroke, myocardial infarct, and death within the periprocedural period or any ipsilateral stroke within 1 year) between carotid endarterectomy (CEA) and CAS patients (CEA: 6.8%, CAS: 7.2%, p=0.51).⁴ Since 96% of CAS patients had embolic protection, CREST can be considered as evidence that the use of DPFs contribute to positive patient outcome. In the updated global CAS registry, Wholey et al.⁵ found that CAS with cerebral protection reduced the stroke and procedure-related deaths from 5.29% to 2.23%. In a review of literature by Kastrup et al.,⁶ the stroke and death rate within 30 days of CAS using cerebral protection was 1.8% as compared to 5.5% without protection.

Various studies have examined the filtration ability of DPFs in both in vitro and ex vivo settings.^{7–12} In addition, previous investigations have noted that DPFs have a negative effect on the local ICA hemodynamics.^{13–15} Our laboratory has evaluated both filtration ability and resistance to flow in an in vitro experimental setup consisting of an ICA flow model under steady and pulsatile flow conditions in the presence of a deployed DPF.^{16–19}

The objective of this investigation was to compare the performance of 6 DPFs on the basis of filtration ability and effects on ICA pressure gradient and vascular impedance. This study is the first to evaluate in vitro performance of the Gore Embolic Filter while maintaining a working fluid temperature of 37°C. By combining pulsatile flow and body temperature conditions, the bench-top flow apparatus described below exhibits the most physiologically realistic conditions for evaluation of endovascular medical devices.

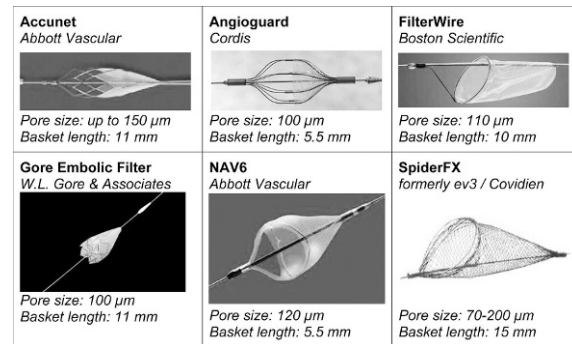


Figure 1 ♦ Distal protection filters used for bench-top testing in this investigation.

METHODS

Experimental Design

Six DPFs (Fig. 1): Accunet (Abbott Vascular, Abbott Park, IL, USA), Angioguard RX (Cordis Corporation, Bridgewater, NJ, USA), FilterWire (Boston Scientific, Natick, MA, USA), Gore Embolic Filter (W.L. Gore & Associates, Flagstaff, AZ, USA), NAV6 (Abbott Vascular), and SpiderFX (ev3/Covidien, Plymouth, MN, USA) were evaluated in a bench-top flow apparatus. Accunet, Angioguard, FilterWire, and SpiderFX have been described previously.^{15,16} Accunet, Angioguard, FilterWire, Gore, and NAV6 have the same basic components: a porous membrane and nitinol frame. Accunet, Angioguard, Gore, and NAV6 have metal struts preceding the basket opening to aid in vessel conformity. FilterWire and SpiderFX have a circumferential ring at the basket opening to conform to the vessel wall. Optimal filtration will be achieved through a combination of DPF-wall apposition, small pore size, and long basket length. Upon retrieval, the DPF opening will collapse into the retrieval catheter, trapping the particulate in the DPF basket. Angioguard and Gore have the smallest pores, while SpiderFX has the largest; SpiderFX has the longest basket length, while Angioguard and NAV6 have the shortest. Figure 1 lists the pore size and basket length of each DPF.

The in vitro flow apparatus previously described^{16–19} was updated for a flow model of a highly curved ICA (Fig. 2A). The justification for this single vessel flow phantom was the desire to test DPF performance in a clinically relevant tortuous ICA where local flow conditions and

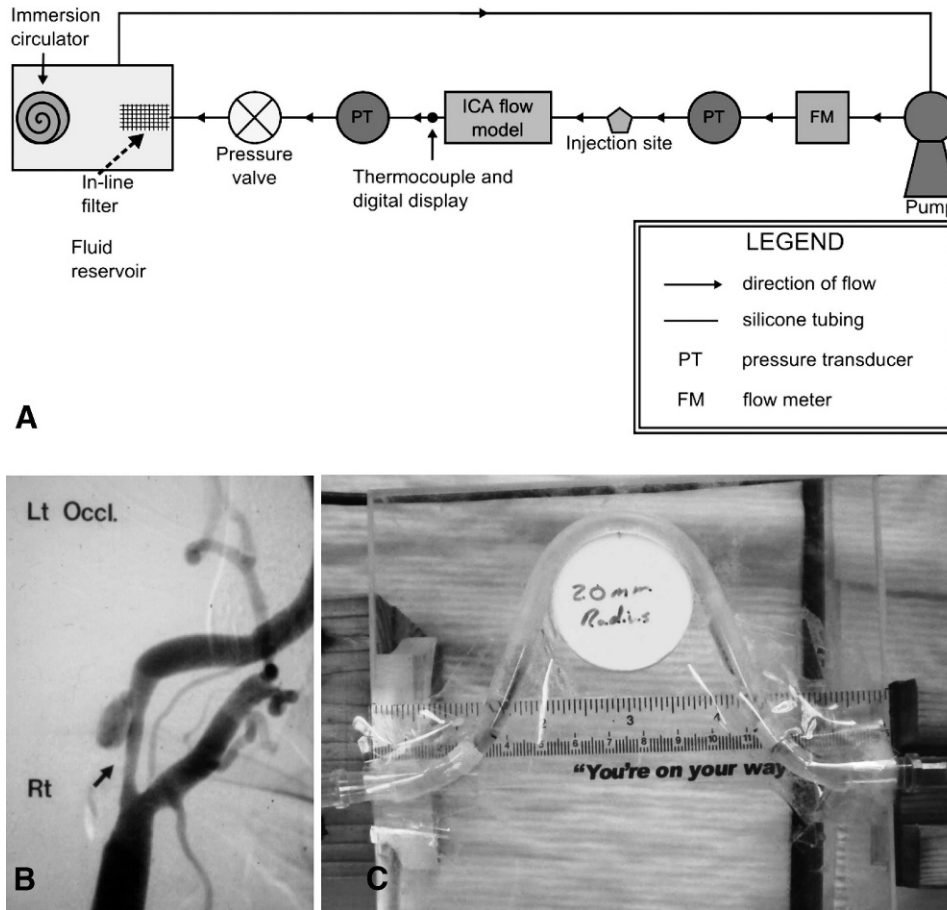


Figure 2 ♦ (A) Schematic of experimental setup, (B) angiogram of a tortuous ICA, and (C) photograph of the ICA flow model.

filter apposition would be challenging (Fig. 2B). A double-acting piston pump (CompuFlow 1000; Shelley Medical Imaging Technologies, Ontario, Canada) output a time-varying flow rate representative of a human ICA.²⁰ The waveform had a period of 0.79 seconds and a time-average flow rate of 205 mL/min. The ICA flow model consisted of a 5.5-mm inner diameter tube having a 20-mm radius of curvature (Fig. 2C). The working fluid was a 40% glycerol solution by volume. An immersion circulator mounted on the external reservoir maintained a working fluid temperature of 37°C.

Pressure transducers (Honeywell, Columbus, OH, USA) were located proximal and distal to the ICA flow model. An electromagnetic flow meter (Seametrics, Kent, WA, USA) was located proximal to the flow model, while a pressure valve (Omega Engineering,

Stamford, CT, USA) was located distal to it. As described previously,¹⁹ the external reservoir was elevated 22 cm to prevent CompuFlow's internal reservoir from emptying. Two different dyed polymer microsphere sizes (ThermoFisher, Waltham, MA, USA), 143 and 200 μm in diameter, were used to simulate plaque debris released during CAS. A syringe probe containing a suspension of 5 mg of microspheres in Tween 20 (ThermoFisher) and water were created for each experiment. Inline filters (Qosina, Edgewood, NY, USA) captured any microspheres missed by the DPFs.

A data acquisition card and in-house LabVIEW program (National Instruments, Austin, TX, USA) acquired pressure and flow rate data at a rate of 200 Hz for 79 seconds, yielding ~ 100 cycles of data at each time point. A pulse output from the pump allowed

for gating of the pressure and flow rate data, which was used for calculation of the average waveforms.

Protocol

After flow stabilization, the pressure and flow rate were acquired [initial conditions (IC)]. The DPF was deployed at the apex of the curved ICA model and pressure and flow rate were measured [empty filter (EF) conditions]. The microspheres were injected into the system and pressure and flow rate were measured a third time [full filter (FF) conditions]. Any microspheres missed by the DPF were captured in the downstream inline filter. After replacing the inline filter with a second filter, the DPF was retrieved. Any microspheres lost during retrieval of the device were captured in the second inline filter. Each experiment was repeated 10 times for each device and each particle size, totaling 120 experiments.

Capture Efficiency, Pressure Gradient, and Vascular Impedance

The mass of particles remaining in the syringe, missed by the DPF, and lost during DPF retrieval were quantified to calculate the filtration ability (capture efficiency) and the percentage of particles lost during retrieval. Capture efficiency was calculated using Equations (1) and (2), where total mass = 5.0 mg:

$$\text{Capture Efficiency} = 100 - \text{Percentage Particles Missed} \quad (\text{Eqn. 1})$$

$$\text{Percentage Particles Missed} = 100 \times \frac{\text{Mass Missed by DPF}}{\text{Total Mass} - \text{Mass Left in Syringe}} \quad (\text{Eqn. 2})$$

The ideal capture efficiency is 100%. The percentage of particles lost during filter retrieval was calculated using Equations (3) and (4):

$$\text{Percentage Particles Lost} = 100 \times \frac{\text{Mass Particles Lost}}{\text{Total Mass Injected} - \text{Mass Missed by DPF}} \quad (\text{Eqn. 3})$$

$$\text{Total Mass Injected} = \text{Total Mass} - \text{Mass Left in Syringe} \quad (\text{Eqn. 4})$$

Conversely, the ideal percentage of particles lost is 0%. The total capture efficiency took into account both the particles captured after injection and the particles lost during retrieval, calculated using Equation (5):

$$\text{Total Capture Efficiency} = 100 - 100 \times \frac{\text{Mass Missed by DPF} + \text{Mass Particles Lost}}{\text{Total Mass Injected}} \quad (\text{Eqn. 5})$$

If all particles were retained, then total capture efficiency equals capture efficiency.

The time-average pressure gradient was calculated for IC, EF, and FF for all DPFs and particle sizes. The increases in time-average pressure gradient induced by the presence of the filter and the particles were computed using Equations (6) and (7):

$$\% \text{ normalized pressure gradient due to filter} = 100 \times \frac{\Delta P_{EF} - \Delta P_{IC}}{\Delta P_{IC}} \quad (\text{Eqn. 6})$$

$$\% \text{ normalized pressure gradient due to particles} = 100 \times \frac{\Delta P_{FF} - \Delta P_{EF}}{\Delta P_{EF}} \quad (\text{Eqn. 7})$$

The time-average waveforms of pressure and flow rate were calculated for IC, EF, and FF conditions. The vascular impedance was calculated proximal and distal to the DPF using Equation (8), as described previously²¹:

$$Z(\omega) = \frac{|P(\omega)|}{|Q(\omega)|}, \quad (\text{Eqn. 8})$$

where Z is the input impedance modulus, $|P|$ is the modulus of the pressure spectrum, and $|Q|$ is the modulus of the flow spectrum. The ideal vascular impedance would remain the same in all 3 conditions.

Statistical Analysis

A 1-way analysis of variance (ANOVA) was executed to compare the mean capture efficiency, pressure gradient, normalized pressure gradient, and vascular impedance of each DPF

for each mass of particles injected. In addition, Tukey’s pairwise comparison was applied with a 95% family confidence interval (CI) to identify performance differences between the DPFs. The significance level was 0.05. All calculations were performed using Minitab (version 16; Minitab Inc., State College, PA, USA).

RESULTS

Capture Efficiency

Capture efficiency was lower for the 143- μ m particles than for the 200- μ m particles for all filters. Gore had the highest capture efficiency for both sizes (99.97% for 143- μ m and 100.00% for 200- μ m particles) and Spider had the lowest (1.50% for 143- μ m and 19.34% for 200- μ m particles). Overall, Filter-Wire and NAV6 had the second and third best overall capture efficiencies for the 143- μ m and 200- μ m particles (FilterWire: 85.38% and 93.43%, NAV6: 63.44% and 97.19%, respectively), followed by Accunet (31.79% and 79.71%, respectively), Angioguard (25.99% and 40.79%, respectively), and Spider (Fig. 3). The Gore filter was the only filter to retain all particles during device retrieval for both particle sizes. During testing of Spider with 143- μ m particles, no particles were observed in the filter basket after retrieval, thus, the percentage of particles lost during retrieval was equal to 100%.

For 143- μ m particles, ANOVA indicated a significant difference in the mean capture efficiency rates among the DPFs ($p < 0.0005$, $F_5 = 246.38$). Tukey’s pairwise comparison identified that all filters were statistically significantly different from each other except Accunet and Angioguard at the $\alpha = 0.05$ level. For 200- μ m particles, ANOVA indicated a significant difference in the mean capture efficiencies among the filters ($p < 0.0005$, $F_5 = 225.33$), while Tukey’s pairwise comparison indicated that Gore, NAV6, and FilterWire were not statistically significantly different from each other at the $\alpha = 0.05$ level.

Flow Rate and Pressure Gradient

The gated flow rate and pressure data were used to find an average waveform for all

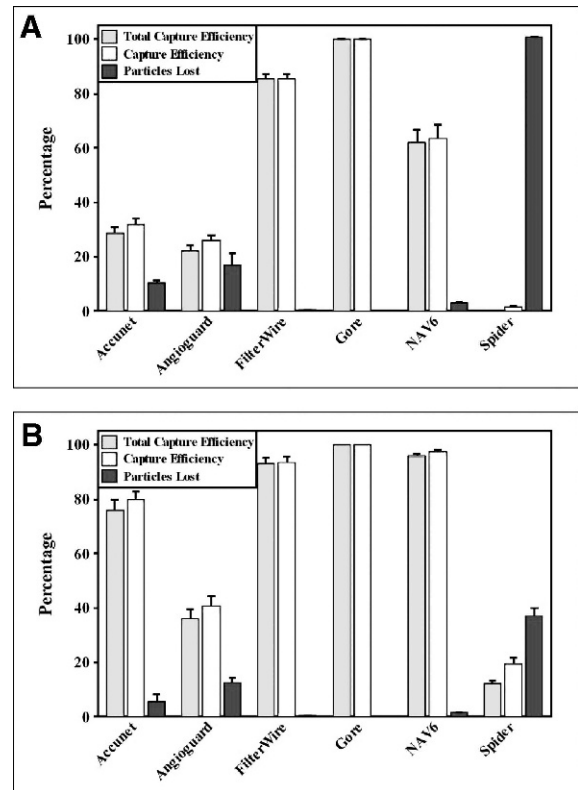


Figure 3 ♦ Average capture efficiency and percentage of particles lost across 10 trials for (A) 143- μ m and (B) 200- μ m particles.

conditions, filters, and particle sizes. NAV6 induced the largest pressure gradient with 143- μ m particles, while Spider had the least effect on pressure gradient even under full filter conditions. It should be noted, however, that Spider also captured the lowest amount of particles. The time average flow rate and pressure data for NAV6 and Spider with 143- μ m are illustrated in Figure 4.

The time-average flow rate and pressure gradient were calculated for IC, EF, and FF for all filters and both particle sizes (Fig. 5). The time-average flow rate was approximately the same regardless of test condition, as expected, but the time-average pressure gradient in the FF condition was greater after injected with 143- μ m particles for Angioguard, FilterWire, and NAV6 as compared with 200- μ m particles. The time-average pressure gradient with 143- μ m particles in the FF condition was lower for Accunet and Gore than with 200- μ m particles. The FF condition time-average pressure

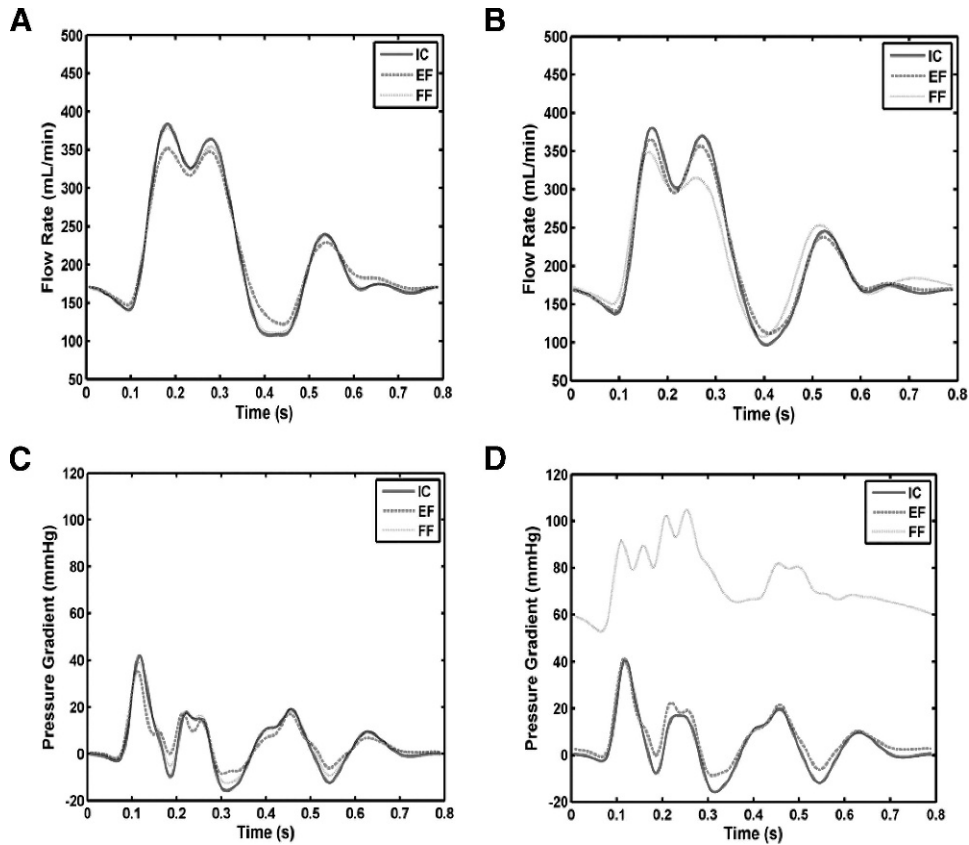


Figure 4 ♦ Best performing EPD (Spider with 143- μm particles) for (A) flow rate and (B) pressure gradient. Worst performing EPD (NAV6 with 143- μm particles) for (C) flow rate and (D) pressure gradient.

gradient was approximately the same for Spider regardless of particle size (Fig. 5C,D).

ANOVA indicated a significant difference in the pressure gradients among the DPFs in EF for 143- μm particles ($p < 0.0005$, $F_5 = 55.07$). AccUNET induced the largest pressure gradient, followed by NAV6, Angioguard, FilterWire, Gore, and Spider ($\Delta P_{EF} - \Delta P_{IC}$). Tukey's pairwise comparison indicated that AccUNET and Angioguard were significantly different, followed by FilterWire, NAV6, and Gore as not significantly different, followed by Spider. Similarly, a significant difference in the EF pressure gradients was seen for 200- μm particles ($p < 0.0005$, $F_5 = 101.50$). Tukey's pairwise comparison indicated that AccUNET was significantly different, followed by Angioguard, NAV6, and FilterWire as not significantly different from each other at the $\alpha = 0.05$ level, followed by Gore, then Spider.

When injected with 143- μm particles, the pressure gradient increase was highest for the NAV6, followed by FilterWire, AccUNET, Angioguard, Gore, and Spider ($\Delta P_{FF} - \Delta P_{EF}$). The DPFs were significantly different from each other ($p < 0.0005$, $F_5 = 31.04$). At the $\alpha = 0.05$ significance level, NAV6 had a significantly greater increase than the other DPFs, followed by AccUNET, FilterWire, and Angioguard, then followed by Gore and Spider.

When injected with 200- μm particles, the pressure gradient increase was highest for AccUNET and NAV6, followed by equal performances of Angioguard, Gore, and FilterWire, and finally Spider ($\Delta P_{FF} - \Delta P_{EF}$). The pressure gradient induced by the injection of 200- μm particles was significantly different for the DPFs ($p < 0.0005$, $F_5 = 48.77$). AccUNET was significantly different from all other DPFs, followed by NAV6, Angioguard, FilterWire,

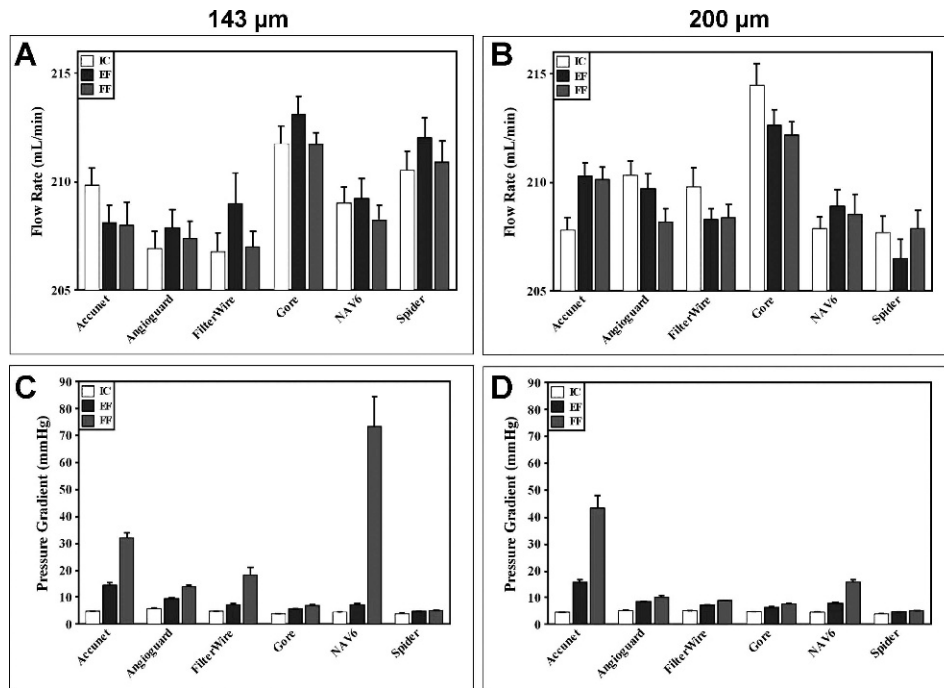


Figure 5 ♦ Time-average flow rate in IC, EF, and FF conditions for (A) 143- μm and (B) 200- μm particles. Time-average pressure gradient in IC, EF, and FF conditions for (C) 143- μm and (D) 200- μm particles.

and Gore, which were not significantly different from each other, then Spider. The normalized percentage time-average pressure gradient increase for 200- μm particles was larger for the Accunet filter, while for the other filters it was larger for the 143- μm particles. Spider had the same normalized percentage pressure gradient for both particle sizes (Fig. 6).

Vascular Impedance

The vascular impedance was calculated by applying the inverse discrete Fourier transform to the ratio of the pressure to the flow rate waveform. The results reported in Figure 7 are the average difference between the proximal and distal vascular impedance real values. The phase angle, or imaginary portion of the vascular impedance, was not reported because in all instances it was nearly zero ($\geq 10^{-17}$ order of magnitude), indicating that pressure and flow rate were nearly exactly in phase with each other. This result was expected due to the use of rigid tubing in the flow apparatus to minimize the difference

between the pulsatile waveform output by the pump and that measured by the flow meter. In the FF condition with 143- μm particles, Angioguard had the highest vascular impedance, followed by Accunet, NAV6, FilterWire, Spider, and Gore. They were not significantly different from each other at the $\alpha=0.05$ level. For 200- μm particles, Accunet had the highest vascular impedance, followed by NAV6, FilterWire, Angioguard, Gore, and Spider. Accunet was significantly greater than all other DPFs ($p<0.0005$, $F_5=9.25$).

DISCUSSION

The current study evaluates 6 DPFs in a physiologically realistic flow apparatus using pulsatile flow rate, 2 particle sizes, and a working fluid heated to body temperature. In this study, the Gore filter retained all particles during retrieval of the device. Gore's capture efficiency was significantly greater than all other filters for 143- μm particles ($p<0.0005$), but was not different from either NAV6 or FilterWire for 200- μm particles. Spider's capture efficiency was significantly less for both

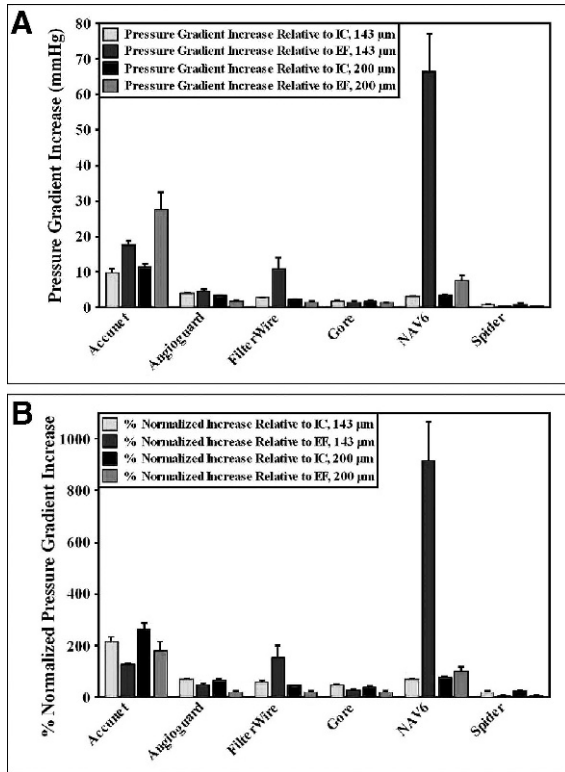


Figure 6 ♦ Time-average pressure gradient increase and normalized percentage pressure gradient increase for (A) 143-µm and (B) 200-µm particles.

particle sizes. Gore and Spider consistently induced the lowest pressure gradient and vascular impedance in EF and FF for both particle sizes. In FF, the pressure gradients for Gore and Spider were not significantly different even though the Gore filter captured nearly all of the particles and the Spider device missed the most particles.

Previously, we quantified the filtration ability of several DPFs and their effect on local flow conditions.^{16–19} We found that DPFs have a high ability to capture particulates that are larger than the pore size of the filter basket, which is typically 100 µm for most DPFs. In a study with particles ranging from 297 to 1000 µm under steady flow conditions, Accunet, FilterWire, and Angioguard achieved capture efficiencies of 99.8%, 99.4%, and 89.1%, respectively.¹⁶ The flow model was a curved 5.5-mm inner diameter tube with ~35° angle between the segments proximal and distal to the apex. In comparison, the current

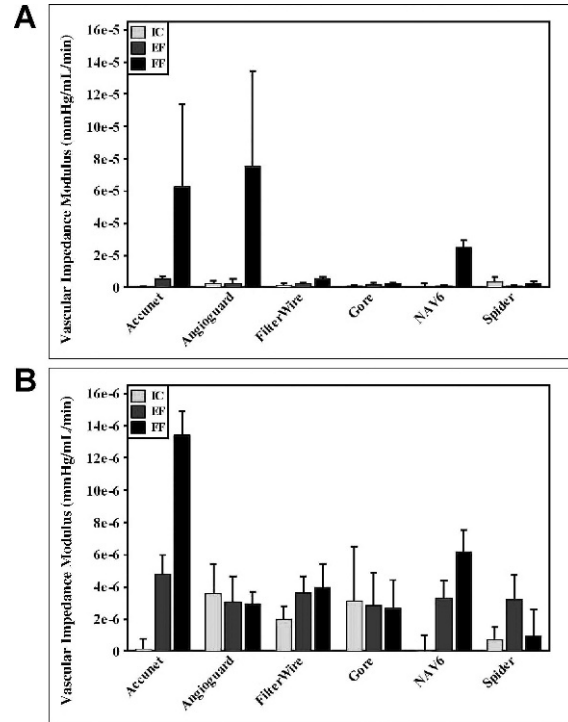


Figure 7 ♦ Average vascular impedance modulus for (A) 143-µm and (B) 200-µm particles.

study used the same 5.5-mm inner diameter tubing with an ~48° angle between the proximal and distal segments under pulsatile flow conditions with a blood analog solution at body temperature. Müller-Hülsbeck et al.^{7–11} conducted several in vitro studies measuring the filtration ability of microspheres and human plaque in steady flow conditions. All of the particulates used in their studies were larger than the DPF pore size and yielded similar results.

For particulates that are approximately the same size as the pore size of the filter basket or smaller, the filtration ability of DPFs is severely limited. This phenomenon is evident in the present study in the case of the Spider, which had a capture efficiency of 1.50% with 143-µm particles and then lost them all upon retrieval of the device. Conversely, in earlier studies we conducted using 300-µm particles, Spider captured 99.9% of the particulates.^{17,18} Particulates ~100 µm in size are large enough to occlude the smaller cerebral arterioles, making the filtration of 143-µm particles all the more clinically relevant.

The trend toward capture efficiency increasing concomitantly with the size of the particulate has also been seen in pulsatile flow experiments. In a previous study conducted by our laboratory, 4 DPFs were injected with particulates ranging in size from 40 to 900 μm . The DPFs had the poorest filtration performance with small particles (40–120 μm) in comparison to particles larger than the pore size (medium: 300–500 μm , large: 700–900 μm).

Reduction in antegrade flow due to the presence of a DPF and filter pores obstructed by plaque emboli can occur in as many as 31% of cases.²² The flow reduction can also contribute to higher adverse outcome rates. Patients with a visible reduction in antegrade flow had a higher incidence of stroke or death within 30 days of CAS (9.5% vs. 2.9%, $p=0.03$).¹³ Similarly, another study found a higher incidence of stroke in flow-impaired cases compared to normal flow cases (8.0% vs. 1.1%, $p=0.11$).¹⁵ Thus, DPFs that minimize the effect on local hemodynamics may have the most desirable clinical outcome. The vascular impedance calculation expresses the effect a DPF has on both pressure and flow rate using a single metric. Furthermore, previous studies have found increased levels of impedance are correlated with reductions in cerebral blood flow velocity,²³ which has implications for ischemic stroke in CAS patients.

In the current study, Accunet induced the largest pressure gradient of all the DPFs, followed by NAV6, Angioguard, FilterWire, Gore, and Spider. When injected with 143- μm particles, the pressure gradient increased significantly for NAV6; when injected with 200- μm particles, it increased significantly for Accunet. Gore and Spider induced the lowest pressure gradients in both EF and FF, which were not significantly different from each other, while having remarkably different capture efficiencies, indicating the minimal impact caused by a full Gore filter on the global flow conditions. The low pressure gradient induced by Spider has been observed in previous studies.^{14,17,18} Hendriks et al.¹⁴ measured the pressure gradient induced by 4 DPFs in a single-tube setup (distance between pressure transducers was not reported) with an input pressure of 70 mmHg and a flow rate

of 200 mL/min. The smallest pressure gradient was caused by Spider RX (1.65 mmHg), followed by RX Accunet (3.90 mmHg), FilterWire EZ (7.95 mmHg), and Angioguard (8.80 mmHg).

In our previous studies, we quantified vascular resistance in the presence of a DPF.^{17,18} The ICA longitudinal vascular impedance in a carotid bifurcation model has been quantified by our laboratory for 4 DPFs.¹⁹ In the present investigation, Angioguard and Accunet induced the largest vascular impedance for 143- μm and 200- μm particles, respectively ($p<0.05$ for 200 μm), while Gore and Spider induced the smallest vascular impedance for 143- μm and 200- μm particles, respectively (not significant for either size). Previously, FilterWire induced the smallest increase in ICA longitudinal impedance following injection of particles ranging in size from 40 to 900 μm in a carotid bifurcation model.¹⁷

DPF design characteristics influence device performance in vitro. Previously, we quantified pore size, porosity, pore density, and the total pore counts of several DPFs.²⁴ In the current study, all of the DPFs were deployed at the apex of the flow model using the same filter-specific demarcation for all trials. Typically, this demarcation was the opening of the filter basket where the porous portion of the polymer basket begins. In the case of Spider, which does not contain a polymer basket, the demarcation was the opening of the nitinol basket. The apex of the curved flow model has a non-circular cross section, representing a challenging case for the DPFs, which have better filtration performance in straight rather than tortuous vessel segments.^{25,26} DPF-wall apposition is particularly important to capturing particles approximately the size of the filter pore, as was evident in the current study. While the Gore Embolic Filter appears to have a similar diamond-shaped strut design at the opening of the filter basket as Accunet, it uses 2 additional nitinol struts along the periphery of the basket opening, which deploy adequately with body temperature to conform to the vessel wall. Accunet, Angioguard, and NAV6 have metal struts preceding the filter basket to appose properly against the vessel wall, but they appear to be

too few to properly conform to non-circular cross sections. Spider and FilterWire have a circular metal ring at the basket opening, which also cannot conform perfectly to a non-circular cross section.²³ In addition, Gore may have performed better than the other DPFs due to a unique combination of relatively small pore size (100 μm), deep filter basket (11 mm), and excellent wall apposition resulting from conformation of its nitinol frame to the vessel wall at body temperature.

To our knowledge, filter volume has not been quantified before; however, Quan et al.²⁷ previously measured the volume of captured particulates during CAS, which was reported as large as 7.57 mm^3 . Based on reported microsphere density (1.06 g/cm^3), the volume of 5 mg of microspheres is 4.72 mm^3 . From this perspective, 4.72 mm^3 would not overwhelm the basket of any DPF, and the capture efficiency reported herein reflects the true capacity of the DPF basket. Furthermore, since all DPFs treat the same vessel size, basket length can give an indication of the relative DPF basket volume.

Not surprisingly, DPFs with high capture efficiencies measured *in vitro* are associated with favorable patient outcome following CAS.²⁸ From that perspective, we would expect Gore and FilterWire to have the best clinical results according to the results of the current investigation. NAV6 has reasonable capture efficiency, especially for large particles, but induces a high pressure gradient. Angioguard, Accunet, and Spider have less desirable bench-top performances.

Most of the DPFs evaluated in this investigation have published clinical trials or pre- or post-market surveillance studies. Gore reported a 1.2% major stroke and death rate in the EMBOLDEN (The GORE EMBOLic Filter in CarotiD StENTing for High Risk Surgical Subjects) trial within 30 days of CAS.²⁹ The BEACH (Boston Scientific EPI: A Carotid Stenting Trial for High-Risk Surgical Patients) trial, a registry for patients undergoing protected CAS with FilterWire EX/EZ, reported a 2.5% 30-day major stroke and death rate in the “pivotal” group; in the subset of patient data reported to the FDA, the rate was 2.7%.³⁰ In CABERNET (Carotid Artery Revascularization Using the Boston Scientific FilterWire

and the EndoTex NexStent), the investigators found a 1.8% 30-day major stroke and death rate.³¹ NAV6’s premarket approval registry, PROTECT (PROTECTed Carotid Artery Stenting in Subjects at High Risk for Carotid Endarterectomy), had a composite stroke or death rate of 0.5% within 30 days of CAS.³² In CASES-PMS (Carotid Artery Stenting With Embolic Protection Surveillance Post-Marketing Study), Angioguard XP was used as the DPF. The 30-day major stroke and death rate was 2.1%.³³ The ARChER (ACCULINK for Revascularization of Carotid in High-Risk patients) trial, which used Accunet, had a 30-day major stroke and death rate of 3.6%.³⁴ The CAPTURE (Carotid Acculink/Accunet Post Approval Trial to Uncover Unanticipated Rare Events) trial also examined the use of RX Accunet, reporting a 30-day major stroke and death rate of 2.9%³⁵; the preliminary results of CAPTURE 2 yielded a 30-day major stroke and death rate of 1.7%.³⁶ The CREATE PAS (Carotid Revascularization With ev3 Arterial Technology Evolution Post Approval Study), which evaluates SpiderFX, is ongoing. However, in CREATE (Carotid Revascularization with ev3 Arterial Technology Evolution), the 30-day major stroke and death rate was 5.5% for its predecessor SpiderRX.³⁷ With the exception of NAV6’s PROTECT trial, the Gore filter’s EMBOLDEN study proved to have a superior 30-day major stroke and death rate.

Conclusion

The present investigation evaluated the *in vitro* performance of 6 DPFs to capture 143- μm and 200- μm particles and their effects on pressure gradient, normalized pressure gradient, and vascular impedance in a highly curved flow model with challenging wall apposition requirements. The presence of physiologically realistic ICA pulsatile flow conditions and the use of a blood analog at body temperature were significant improvements to the protocol compared to our previous work. According to the analysis of the 4 relevant experimental parameters, the Gore Embolic Filter appears to have the best wall apposition of the devices tested and should be able to capture plaque particulate in tortuous carotid anatomies. The Gore filter

had high capture efficiencies with relatively small effects on local pressure gradient and vascular impedance. FilterWire and NAV6 had equally significant capture efficiencies when used with 200- μ m particles. Spider had the least effect on pressure gradient and vascular impedance, an outcome likely related to the larger pore sizes of its metal basket.

REFERENCES

1. Tan WA, Bates MC, Wholey MH. Cerebral protection systems for distal emboli during carotid artery interventions. *J Interv Cardiol*. 2001;14:465–474.
2. Bates ER, Babb JD, Casey DE, et al. ACCF/SCAI/SVMB/SIR/ASITN 2007 clinical expert consensus document on carotid stenting: a report of the American College of Cardiology Foundation Task Force on Clinical Expert Consensus Documents (ACCF/SCAI/SVMB/SIR/ASITN Clinical Expert Consensus Document Committee on Carotid Stenting). *J Am Coll Cardiol*. 2007;49:126–170.
3. Barbato JE, Dillavou E, Horowitz MB, et al. A randomized trial of carotid artery stenting with and without cerebral protection. *J Vasc Surg*. 2008;47:760–765.
4. Brott TG, Hobson RW, Howard G, et al. Stenting versus endarterectomy for treatment of carotid-artery stenosis. *N Engl J Med*. 2010;363:11–23.
5. Wholey MH, Al-Mubarak N, Wholey MH. Updated review of the global carotid artery stent registry. *Catheter Cardiovasc Interv*. 2003;60:259–266.
6. Kastrup A, Groschel K, Krapf H, et al. Early outcome of carotid angioplasty and stenting with and without cerebral protection devices: a systematic review of the literature. *Stroke*. 2003;34:813–819.
7. Charalambous N, Jahnke T, Bolte H, et al. Reduction of cerebral embolization in carotid angioplasty: an in-vitro experiment comparing 2 cerebral protection devices. *J Endovasc Ther*. 2009;16:161–167.
8. Müller-Hülsbeck S, Grimm J, Liess C, et al. Comparison and modification of two cerebral protection devices used for carotid angioplasty: in vitro experiment. *Radiology*. 2002;225:289–294.
9. Müller-Hülsbeck S, Husler EJ, Schaffner SR, et al. An in vitro analysis of a carotid artery stent with a protective membrane. *J Vasc Interv Radiol*. 2004;15:1295–1305.
10. Müller-Hülsbeck S, Jahnke T, Liess C, et al. Comparison of various cerebral protection devices used for carotid artery stent placement: an in vitro experiment. *J Vasc Interv Radiol*. 2003;14:613–620.
11. Müller-Hülsbeck S, Jahnke T, Liess C, et al. In vitro comparison of four cerebral protection filters for preventing human plaque embolization during carotid interventions. *J Endovasc Ther*. 2002;9:793–802.
12. Ohki T, Roubin GS, Veith FJ, et al. Efficacy of a filter device in the prevention of embolic events during carotid angioplasty and stenting: an ex vivo analysis. *J Vasc Surg*. 1999;30:1034–1044.
13. Casserly IP, Abou-Chebl A, Fathi RB, et al. Slow-flow phenomenon during carotid artery intervention with embolic protection devices: predictors and clinical outcome. *J Am Coll Cardiol*. 2005;46:1466–1472.
14. Hendriks JM, Zindler JD, van der Lugt A, et al. Embolic protection filters for carotid stenting: differences in flow obstruction depending on filter construction. *J Endovasc Ther*. 2006;13:47–50.
15. Roffi M, Greutmann M, Schwarz U, et al. Flow impairment during protected carotid artery stenting: impact of filter device design. *J Endovasc Ther*. 2008;15:103–109.
16. Finol EA, Siewiorek GM, Scotti CM, et al. Wall apposition assessment and performance comparison of distal protection filters. *J Endovasc Ther*. 2008;15:177–186.
17. Siewiorek GM, Wholey MH, Finol EA. In vitro performance assessment of distal protection devices for carotid artery stenting: effect of physiological anatomy on vascular resistance. *J Endovasc Ther*. 2007;14:712–724.
18. Siewiorek GM, Wholey MH, Finol EA. Vascular resistance in the carotid artery: an in vitro investigation of embolic protection filters. *J Vasc Interv Radiol*. 2008;19:1467–1476.
19. Siewiorek GM, Wholey MH, Finol EA. In vitro performance assessment of distal protection filters: pulsatile flow conditions. *J Endovasc Ther*. 2009;16:735–743.
20. Holdsworth DW, Norley CJ, Frayne R, et al. Characterization of common carotid artery blood-flow waveforms in normal human subjects. *Physiol Meas*. 1999;20:219–240.
21. Weinberg CE, Hertzberg JR, Ivy DD, et al. Extraction of pulmonary vascular compliance, pulmonary vascular resistance, and right ventricular work from single-pressure and Doppler flow measurements in children with pulmonary hypertension: a new method for evaluating reactivity: in vitro and clinical studies. *Circulation*. 2004;110:2609–2617.

22. Castellani L, Causin F, Danieli D, et al. Carotid stenting with filter protection. Correlation of ACT values with angiographic and histopathologic findings. *J Neuroradiol.* 2003;30:103–108.
23. Zhu YS, Tseng BY, Shibata S, et al. Increases in cerebrovascular impedance in older adults. *J Appl Physiol.* 2011;111:376–381.
24. Siewiorek GM, Eskandari MK, Finol EA. The Angioguard embolic protection device. *Expert Rev Med Devices.* 2008;5:287–296.
25. Order BM, Glass C, Liess C, et al. Comparison of 4 cerebral protection filters for carotid angioplasty: an in vitro experiment focusing on carotid anatomy. *J Endovasc Ther.* 2004;11:211–218.
26. Shah AR, Lipsitz EC, Scher L, et al. The effect of tortuosity on five different cerebral protection devices in an ex-vivo model. Presented at the Eastern Vascular Society; September 24–26, 2009; Philadelphia, Pennsylvania, USA.
27. Quan VH, Huynh R, Seifert PA, et al. Morphometric analysis of particulate debris extracted by four different embolic protection devices from coronary arteries, aortocoronary saphenous vein conduits, and carotid arteries. *Am J Cardiol.* 2005;95:1415–1419.
28. Siewiorek GM, Krafty RT, Wholey MH, et al. The association of clinical variables and filter design with carotid artery stenting thirty-day outcome. *Eur J Vasc Endovasc Surg.* 2011;42:282–291.
29. Gray WA. The Gore EMBOLDEN clinical study. Presented at Vascular Interventional Advances (VIVA); October 19–22, 2010; Las Vegas, Nevada, USA.
30. White CJ, Iyer SS, Hopkins LN, et al. Carotid stenting with distal protection in high surgical risk patients: the BEACH trial 30 day results. *Catheter Cardiovasc Interv.* 2006;67:503–512.
31. Hopkins LN, Myla S, Grube E, et al. Carotid artery revascularization in high surgical risk patients with the NexStent and the FilterWire EX/EZ: 1-year results in the CABERNET trial. *Catheter Cardiovasc Interv.* 2008;7:950–960.
32. Chaturvedi S, Gray WA, Matsumura J. Safety outcomes from the PROTECT Carotid Artery Stenting Multicenter Study. Presented at the International Stroke Conference; February 17–20, 2009; San Diego, California, USA.
33. Katzen BT, Criado FJ, Ramee SR, et al. Carotid artery stenting with emboli protection surveillance study: thirty-day results of the CASES-PMS study. *Catheter Cardiovasc Interv.* 2007;70:316–323.
34. Gray WA, Hopkins LN, Yadav S, et al. Protected carotid stenting in high-surgical-risk patients: the ARChER results. *J Vasc Surg.* 2006;44:258–268.
35. Fairman R, Gray WA, Scicli AP, et al. The CAPTURE registry: analysis of strokes resulting from carotid artery stenting in the post approval setting: timing, location, severity, and type. *Ann Surg.* 2007;246:551–558.
36. Gray WA, Chaturvedi S, Verta P, et al. Thirty-day outcomes for carotid artery stenting in 6320 patients from 2 prospective, multicenter, high-surgical-risk registries. *Circ Cardiovasc Interv.* 2009;2:159–166.
37. Safian RD, Bresnahan JF, Jaff MR, et al. Protected carotid stenting in high-risk patients with severe carotid artery stenosis. *J Am Coll Cardiol.* 2006;47:2384–2389.

◆ COMMENTARY

Experimental, Ex Vivo, and Bench Testing to Evaluate Embolic/Distal Protection Devices: Useful or Wasteful?

Stefan Müller-Hülsbeck, MD, EBIR

Department of Diagnostic and Interventional Radiology / Neuroradiology, Diakonissenanstalt zu Flensburg, Zentrum für Gesundheit und Diakonie, Flensburg, Germany.

To answer the question posed in the title seems rather easy, but before giving an answer, one has to go back to the roots of interventional radiology and endovascular therapy. Basic work in interventional therapy, as with most other therapeutic options, usually starts with schematic drawings,¹ proceeds to self- or handmade prototypes constructed on the bench or in the kitchen,^{2,3} and then ends with a lot of tests in animal models,⁴ accompanied by experimental tests on the bench. This step-by-step process is the common way in which most commercial products are developed and evaluated. Unfortunately, physicians are not well informed about what is happening behind the scenes in the laboratories of our industry partners until an interventional tool gets approved either by the Food and Drug Administration or the European Union [the latter's Conformité Européenne (CE) mark is definitely easier to obtain].

In industry, independent data from the bench are rare; why is that? First, constructing a suitable bench model for dedicated testing of embolic/distal protection devices (E/DPD) is not that easy, largely because one needs both the ideas and the money. Second, these mechanical bench tests are very easy to understand; no dedicated information is needed on bioengineering, gene therapy, or molecular imaging, for example. This latter fact, especially, makes bench tests less amazing and complex, and while their results are easy to follow, their science is not that deep,

some critics would state. Personally, I would say it was the other way around: bench tests, especially when the model is easy to reproduce, generate results that are of utmost importance for providing insight into what can be expected during clinical application. For E/DPDs, these important data are now available.

In this issue of *JEVT*, Siewiorek and coworkers,⁵ as well as other independent research groups,^{6,7} have done some basic work comparing the efficacy of E/DPDs and found performance differences and potential limitations ex vivo. Based on these experiments published in medical journals, improvements in so-called next-generation devices were applied for safer clinical use; in other instances, companies even stopped intended market release.⁸

One has to congratulate the Siewiorek group for their detailed and outstanding flow model mimicking a clinical setting. This bench model for E/DPD testing was improved compared to previous settings from other research groups working on the same topic. The current data obtained from the latest bench tests might be helpful in giving physicians and operators using E/DPDs additional insights as to which device they might use and what they can expect in terms of debris capture efficacy when particulate sizes range from 143 to 200 μm . It would be of great interest to have these competitive, independent data available for every E/DPD that seeks marketing approval.

Invited commentaries published in the *Journal of Endovascular Therapy* reflect the opinions of the author(s) and do not necessarily represent the views of the *Journal* or the INTERNATIONAL SOCIETY OF ENDOVASCULAR SPECIALISTS.

The author has no commercial, proprietary, or financial interest in any products or companies described in this article.

Corresponding author: Stefan Müller-Hülsbeck, MD, EBIR, FCIRSE, FICA, Head, Department of Diagnostic and Interventional Radiology / Neuroradiology, Ev.-Luth. Diakonissenanstalt zu Flensburg, Zentrum für Gesundheit und Diakonie, Knuthstr. 1, 24939 Flensburg, Germany. E-mail: muehue@diako.de

Discussing these data from the bench, a further question arises: are these tests close to reality? The use of pulsatile flow, body temperature, blood viscosity equivalents, and so on is helpful in approaching real clinical scenarios. Nevertheless, even dedicated bench models are both close to and far from reality. Two major factors are missing: the patient (with challenging anatomy and comorbidities) and the operator (with differing skill levels). Therefore, data from the bench have to be extrapolated with greatest care to the clinical situation. However, they are helpful in providing useful information and insight into potential performance differences. In addition, they are able to show potential unmet needs for device improvement in terms of not only capture efficacy but also device placement and retrieval. Unfortunately, insofar as predicting the clinical outcome of an E/DPS design, the differences in efficacy and performance between the model and the clinical setting will remain an impediment.

Bench testing, as performed well by the Siewiorek group, is very useful. Hopefully, their excellent work encourages more physicians to establish bench testing. Referring to the process of creation in the world of endovascular therapy, the philosophy “less is often more” can be translated to “test at the bench before harming patients and make devices easy to understand.” I have the dream that one day this kind of test will be standardized and even a “standard” for endovascular device approval.

Last but not least, the final question remains unanswered as to whether or not E/DPDs should be used on a routine basis in clinical cases; in the SPACE (Stent-Supported Percutaneous Angioplasty of the Carotid Artery vs. Endarterectomy) and the ICSS

(International Carotid Stenting Study) trials, the rates of E/DPD usage were 26% and 72%, respectively.⁹

REFERENCES

1. Seldinger SI. Catheter replacement of the needle in percutaneous arteriography; a new technique. *Acta Radiol.* 1953;39:368–376.
2. Dotter CT, Judkins MP. Transluminal treatment of arteriosclerotic obstruction. description of a new technic and a preliminary report of its application. *Circulation.* 1964;30:654–670.
3. Grüntzig A. [Percutaneous recanalisation of chronic arterial occlusions (Dotter principle) with a new double lumen dilatation catheter (author’s transl)]. *Rofo.* 1976;124:80–86.
4. Palmaz JC, Sibbitt RR, Reuter SR, et al. Expandable intrahepatic portacaval shunt stents: early experience in the dog. *AJR Am J Roentgenol.* 1985;145:821–825.
5. Siewiorek GM, Wholey MH, Finol EA. A comparative analysis of bench-top performance assessment of distal protection filters in transient flow conditions. *J Endovasc Ther.* 2012;19:249–260.
6. Ohki T, Roubin GS, Veith FJ, et al. Efficacy of a filter device in the prevention of embolic events during carotid angioplasty and stenting: an ex vivo analysis. *J Vasc Surg.* 1999;30:1034–1044.
7. Müller-Hülsbeck S, Grimm J, Liess C, et al. Comparison and modification of two cerebral protection devices used for carotid angioplasty: in vitro experiment. *Radiology.* 2002;225:289–294.
8. Charalambous N, Jahnke T, Bolte H, et al. Reduction of cerebral embolization in carotid angioplasty: an in-vitro experiment comparing 2 cerebral protection devices. *J Endovasc Ther.* 2009;16:161–167.
9. Macdonald S. Carotid artery stenting trials: conduct, results, critique, and current recommendations. *Cardiovasc Intervent Radiol.* 2012; 35:15–29.